

Electronic Supplementary Information

Differential Interference Contrast Microscopy Imaging of Micrometer-Long Plasmonic Nanowires

*Ji Won Ha, Kuangcai Chen, and Ning Fang**

Ames Laboratory, U.S. Department of Energy, and Department of Chemistry, Iowa State
University, Ames, Iowa 50011, United States

*To whom correspondence should be addressed. E-mail: nfang@iastate.edu

This document contains the experimental details, additional experimental results and discussion,
Figures S1 to S17, and Movies S1 to S3.

MOVIE

Movie S1

This movie shows rotational motions of Au nanowire 3 (Fig. S10A) with one fixed binding site at its center on the synthetic membrane.

Movie S2

This movie shows rotational motions of Au nanowire 4 (Fig. S10A) with one fixed binding site at the end on the synthetic membrane.

Movie S3

This movie shows rotational motions of Au nanowire 5 (Fig. S10A) with multiple fixed binding sites on the synthetic membrane.

1. Differential Interference Contrast Microscopy

Differential interference contrast (DIC) microscopy was performed with an upright Nikon Eclipse 80i microscope in this study. The DIC mode used a pair of Nomarski prisms, two polarizers, a quarter-wave plate, a Plan Apo oil-immersion objective (100 \times , N.A. = 1.40), and an oil-immersion condenser (N.A. = 1.40). Band-pass filters (520 nm, 550 nm, 640 nm) with a full width at half-maximum (FWHM) of 10 nm were obtained from Thorlab (Newton, NJ, USA) and inserted into the light path in the microscope. A Hamamatsu CMOS camera (ORCA-Flash 2.8) was employed to record highly detailed DIC images of Au nanowires and to record dynamics of Au nanowires rotating on synthetic membranes.

2. The Working Principle of DIC Microscopy to Image Single Au Nanowires

In DIC microscopy the incident beam is split into two orthogonally polarized beams in the two bright (blue-line) and dark (red-line) polarization directions by the first Nomarski prism as shown in Fig. S2. When two beams pass through the specimen, they generate image contrasts for optical path length gradients in the specimen. Therefore, each of the two orthogonally polarized beams generates an independent intermediate image. One such image is shifted laterally by ~ 100 nm and then overlapped with the other to generate the final interference image. For anisotropic shape of Au nanowires, the two intermediate images are different because the two illumination beams are phase-delayed to different extents, depending on the orientation of the Au nanowire relative to the two polarization directions. Therefore, the DIC images of Au nanowires have disproportionate bright and dark parts and they show different bright and dark intensities depending on the Au nanowire orientation.

3. Sample Preparation and DIC Imaging of Au Nanowires

Au nanowires with an average size of 2000 nm × 75 nm were purchased from Nanopartz (A14-2000, Loveland, CO). The Au nanowire colloid solution was first sonicated for 15 min at room temperature. We made a solution containing 80-nm Au nanospheres and the Au nanowires. The 80-nm Au nanospheres were purchased from BBI (WI, USA). A sample was prepared by spin casting the solution on the pre-cleaned glass slide to position the Au nanowires relatively flat to the surface as they were fixed to the slide. Then, a 22 mm × 22 mm No. 1.5 coverslip (Corning, NY) was covered on the glass slide. In this study, the concentration of Au nanowires on the glass surface was controlled to facilitate single particle characterization.

The sample glass slide was placed on a 360° rotating mirror holder affixed onto the microscope stage. By rotating the mirror holder 10° per step, the Au nanowires were positioned in different orientations. The 80-nm Au nanospheres were used as a standard to fix the focal plane after rotating each 10° of the stage. To excite the Au nanowire with different SPR wavelengths, band-pass filters (520 nm, 550 nm, 640 nm) were inserted into the light path in the microscope. DIC images were taken with the Hamamatsu CMOS camera. The collected images and movies were analyzed with MATLAB and NIH ImageJ.

4. Preparation of Synthetic Lipid Bilayers on Glass Slides

The phospholipid 1-palmitoyl-2-oleoyl-sn-glycero-3-phosphocholine (POPC, Avanti Polar Lipids) solution in chloroform was first dried by a nitrogen stream and followed by at least 3 hr drying under vacuum at room temperature to remove the residual chloroform. The dried lipids were stored in a -20°C freezer.

Phosphate buffered saline (1× PBS, pH 7.4) was used to bring the final concentration to 0.5 mg/mL. The cloudy solution containing multilamellar vesicles was obtained after swelling in the PBS buffer solution for 30 min with several times vortexing. The suspension solution was then forcing through a 100 nm pore size polycarbonate membrane at least 21 times to prepare the solution with large unilamellar vesicles using a mini-extruder (Avanti Polar Lipids, Alabaster, AL). The resulted solution was kept in a 4°C fridge.

The planar bilayer was formed by incubating the large unilamellar vesicles solution on a freshly cleaned glass slide in a chamber created by two double-sided tapes and a clean coverslip for 10 min. After that, PBS was used to remove the excess lipids. Au nanowire solution was then introduced into the chamber with the membrane for DIC imaging.

5. DIC Polarization Anisotropy

Although Au nanowires are directly visualized under a DIC microscope (Fig. S12, S13, S14), a faster and more reliable method than eye to analyze their motions dynamically is still required. In this study, we tested if DIC polarization anisotropy can be used as a fast, simple and accurate method to determine the orientations of single Au nanowires. The DIC polarization anisotropy P can be conveniently obtained from the bright and dark intensities of a single DIC image of the Au nanowire.¹ DIC polarization anisotropy using an intensity ratio instead of absolute intensities is less affected by intensity instabilities so that it leads to more accurate, reproducible and reliable angle measurements.^{1, 2} DIC polarization anisotropy is defined in the following equation 1.

$$P = \frac{I_{B,N} - I_{D,N}}{I_{B,N} + I_{D,N}} \quad (1)$$

where $I_{B,N}$ and $I_{D,N}$ are the normalized bright and dark intensities, respectively.

We found that the normalized bright and dark DIC intensities for Au nanowire 2 at 550 nm are anti-correlated and well fitted with functions of $\sin^4(\varphi)$ and $\cos^4(\varphi)$ (Fig. S15A). DIC polarization anisotropy was computed from the orthogonally polarized bright and dark intensities of Au nanowire 2 at 550 nm. Fig. S15B shows the polarization anisotropy P for Au nanowire 2 as a function of orientation angle φ . The P values are in the range of -1 to +1 depending on the Au nanowire's orientation relative to the bright and dark polarization directions as illustrated in Fig. S15B. Since the DIC bright (or dark) intensity of a Au nanowire is proportional to the fourth power of the sine (or cosine) of the orientation angle φ , the P values can be calculated directly for any given φ using the following equation 2.

$$P = \frac{\sin^4(\varphi) - \cos^4(\varphi)}{\sin^4(\varphi) + \cos^4(\varphi)} \quad (2)$$

As shown in Fig. S15B, the experimental P values obtained from equation 1 agree well with the theoretical P values calculated from equation 2. This validates that DIC polarization anisotropy enables accurate measurements of orientation angle of micrometer-long Au nanowires. The orientation angle φ can be deduced backward from the measurement of P values.¹

We further tested if DIC polarization anisotropy can be directly used to track rotational dynamics of individual Au nanowires in a fast dynamic process. Fig. S11 shows DIC intensities of two Au nanowires (3 and 4 in Fig. S10A) rotating on the membrane and their bright and dark

intensities are mostly anti-correlated during the dynamic process. DIC polarization anisotropy for the two nanowires was then computed, and it is observed that the P values for the nanowires are randomly distributed between -1 and 1 as a function of time (Fig. S16). In contrast, Au nanowire 5 (in Fig. S10A) with multiple binding sites show much lower freedom of rotation, and the little movement resulted in the P values fluctuating at around 0.1 as a function of time (Fig. S17). Therefore, we found that the DIC polarization anisotropy can be used as faster and more accurate method than eye to track rotational motions of Au nanowires in dynamic studies.

References

1. J. W. Ha, W. Sun, G. Wang and N. Fang, *Chem. Commun.*, 2011, **47**, 7743-7745.
2. J. W. Ha, W. Sun, A. S. Stender and N. Fang, *J. Phys. Chem. C*, 2012, **116**, 2766-2771.

Supplementary Figures

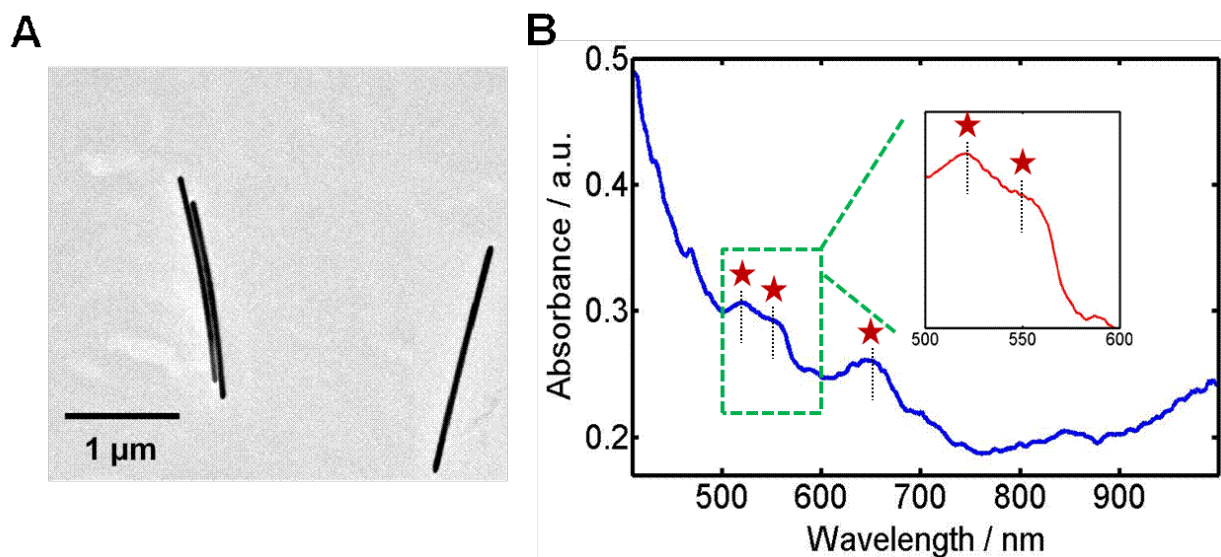


Fig. S1. (A) TEM image of Au nanowires. The average length and width of nanowires are 2000 nm and 75 nm, respectively. (B) UV-Vis absorption spectrum of 2 μm-long Au nanowires dispersed in water. The transverse SPR peak appears at 520 nm, while the prominent higher-order multipolar peaks appear at 550 nm and 640 nm. The three SPR peaks are indicated with a red-star.

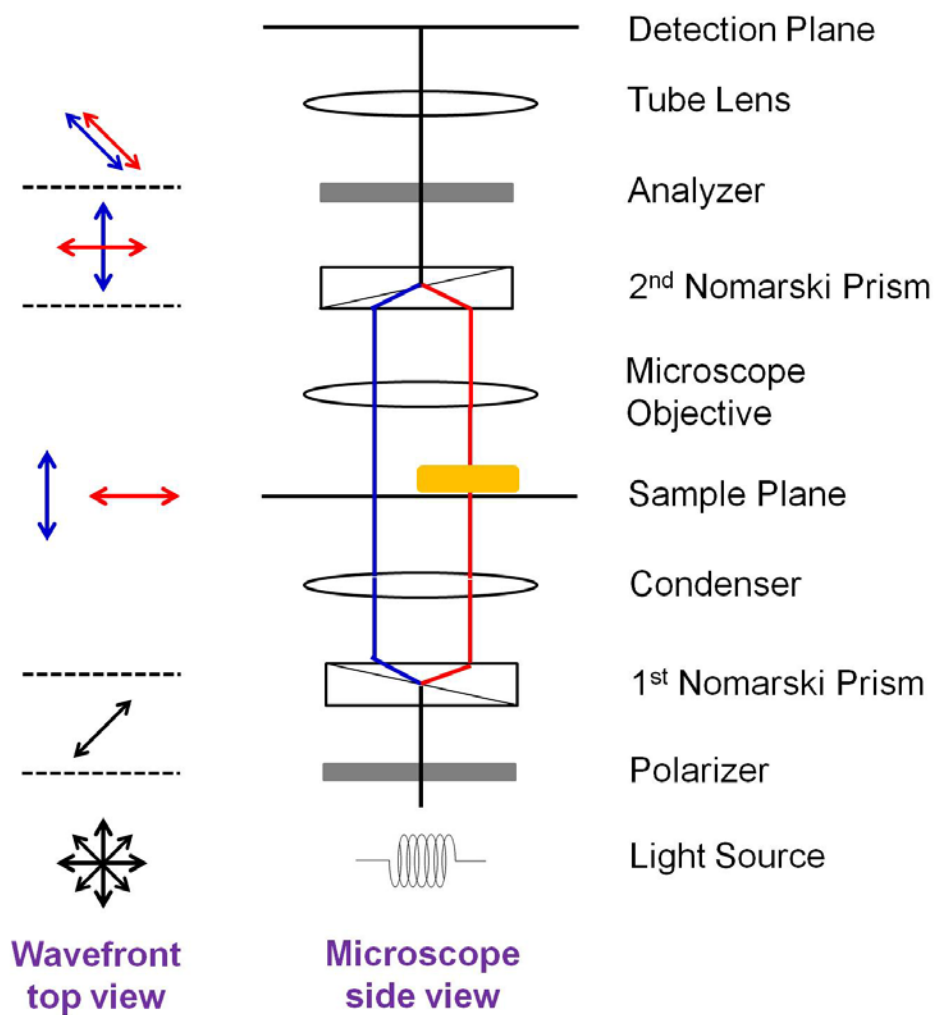


Fig. S2. The optical path and wavefront in the DIC microscope. The blue- and red- lines represent the optical path of two orthogonal beams split by the first Nomarski prism.

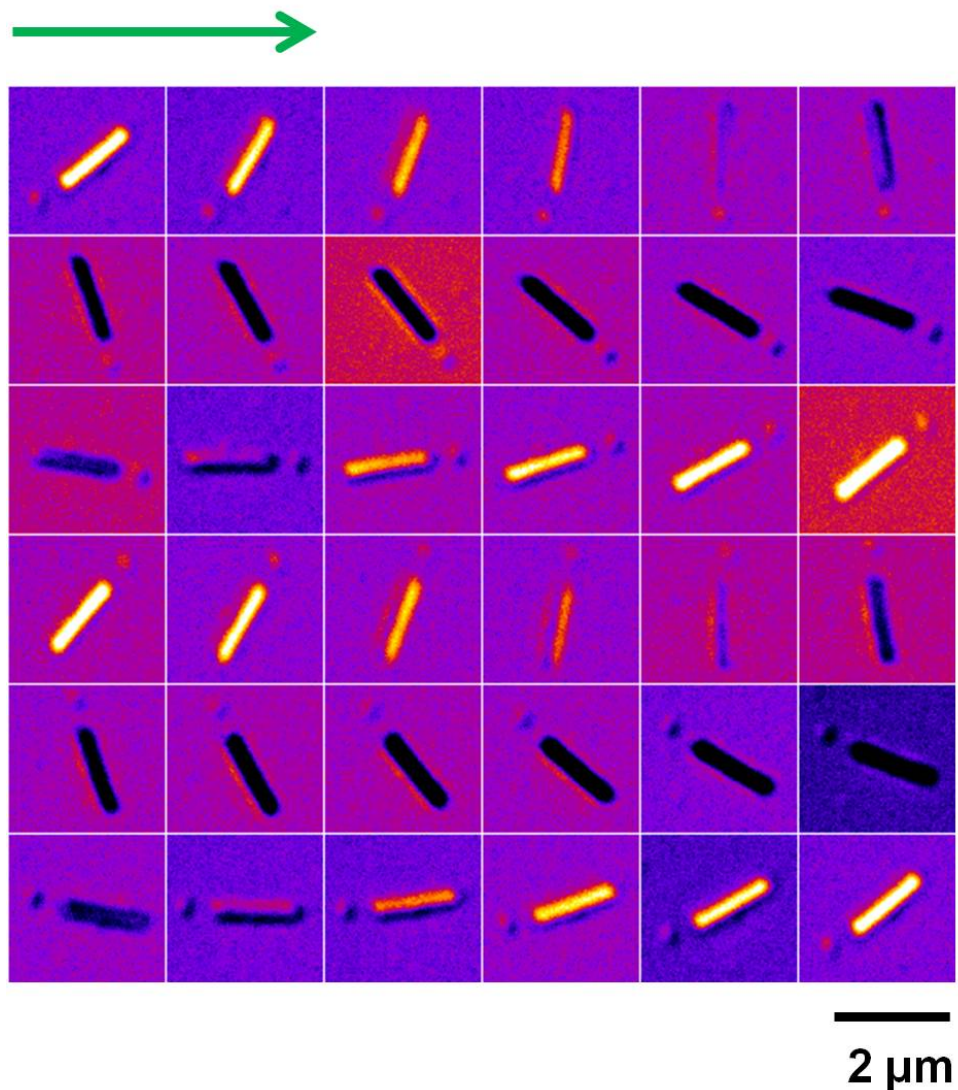


Fig. S3. A complete set of DIC images of Au nanowire 1 in Fig. 1 at 36 orientations from 0° to 360° with an increment of 10° . The nanowire is excited at 520 nm close to its transverse SPR mode. The image patterns are changed periodically as a function of orientation angle.

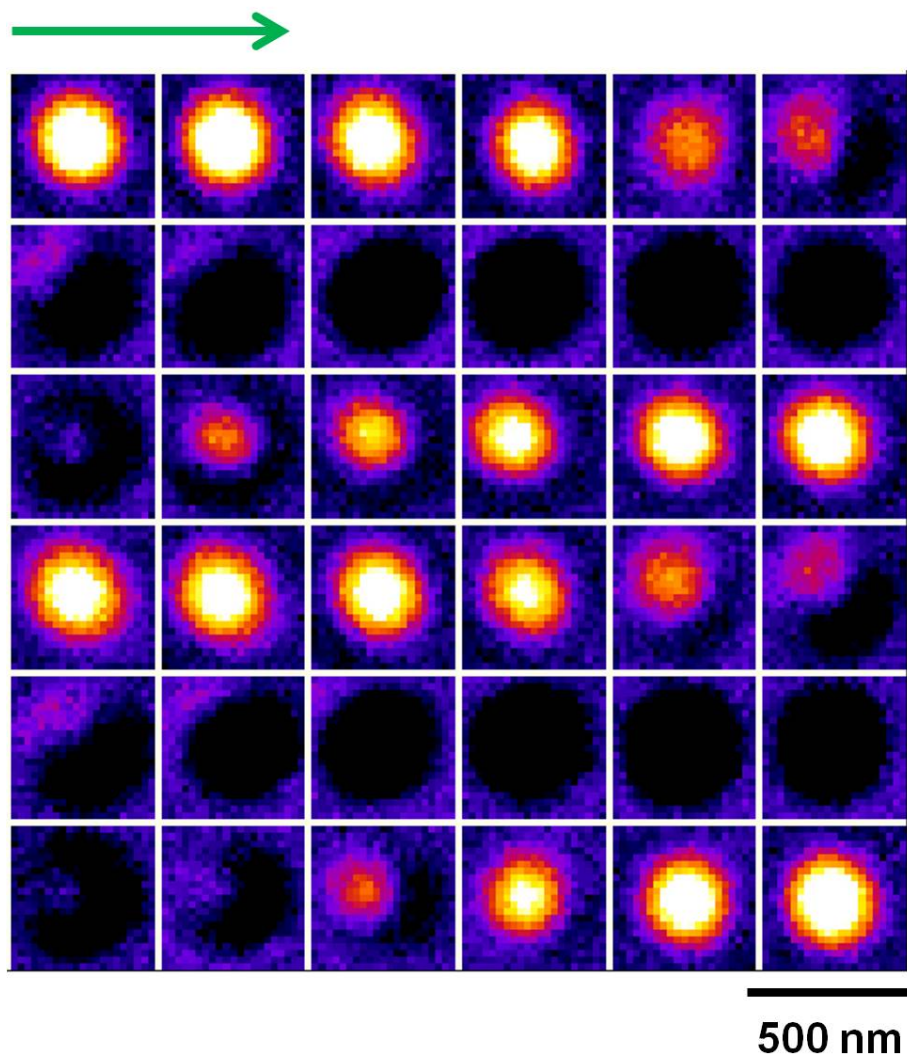


Fig. S4. A complete set of DIC images of single Au nanorod ($25 \text{ nm} \times 73 \text{ nm}$) at 36 orientations from 0° to 360° with an increment of 10° . The nanorod is excited at 700 nm close to its longitudinal SPR mode. The DIC image patterns change periodically as a function of orientation angle.

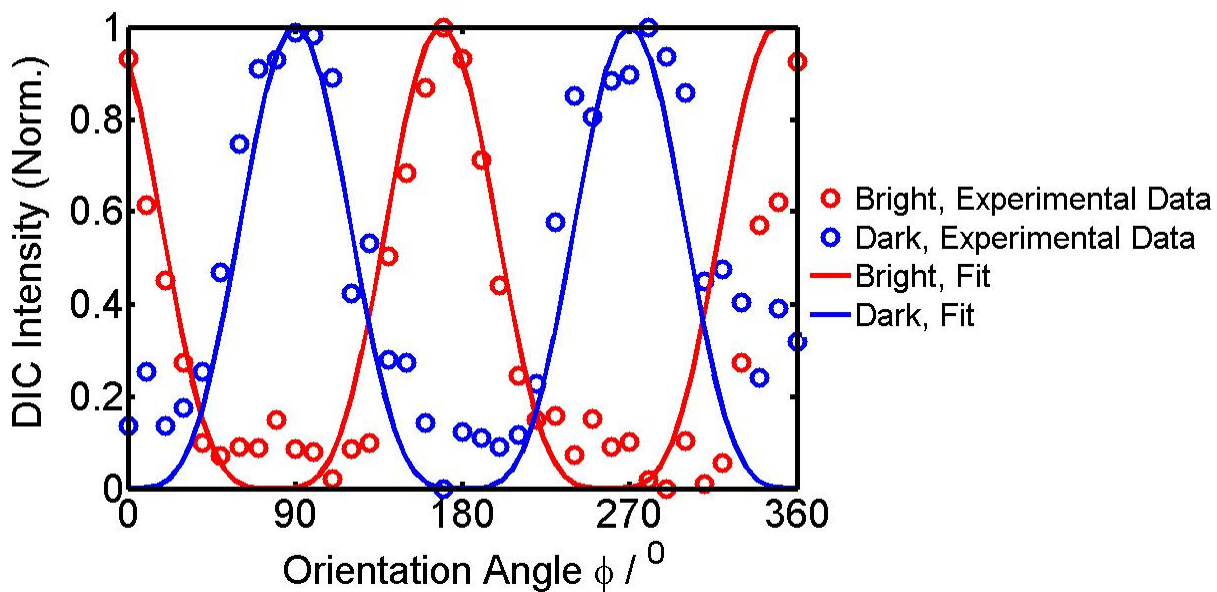


Fig. S5. DIC Intensity profiles of the Au nanowire 1 in Fig. 1 as a function of orientation angle φ . The normalized bright (red-curve) and dark (blue-curve) DIC intensities were fitted with functions of $\sin^2(\varphi)$ and $\cos^2(\varphi)$, respectively.

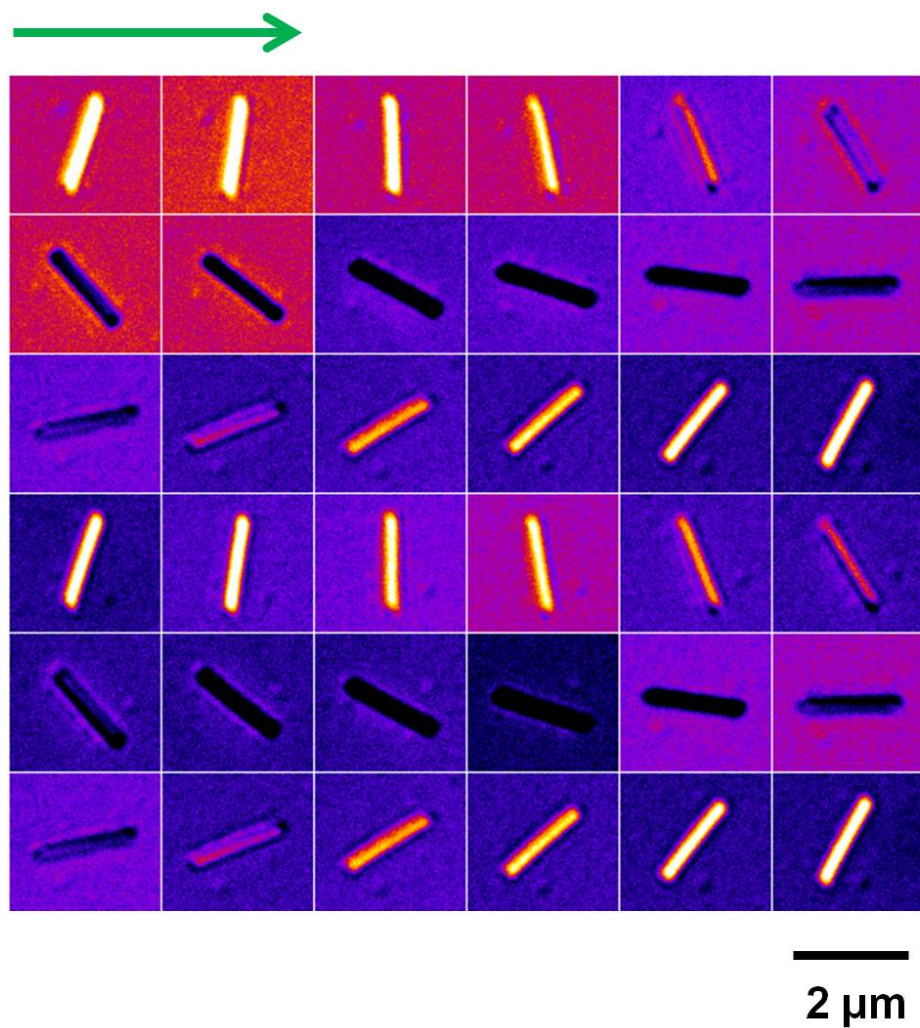


Fig. S6. A complete set of DIC images of the highlighted Au nanowire 2 in Fig. 2. The nanowire is excited at 550 nm. The image patterns are changed periodically as a function of orientation angle φ from 0° to 360° with an increment of 10° .

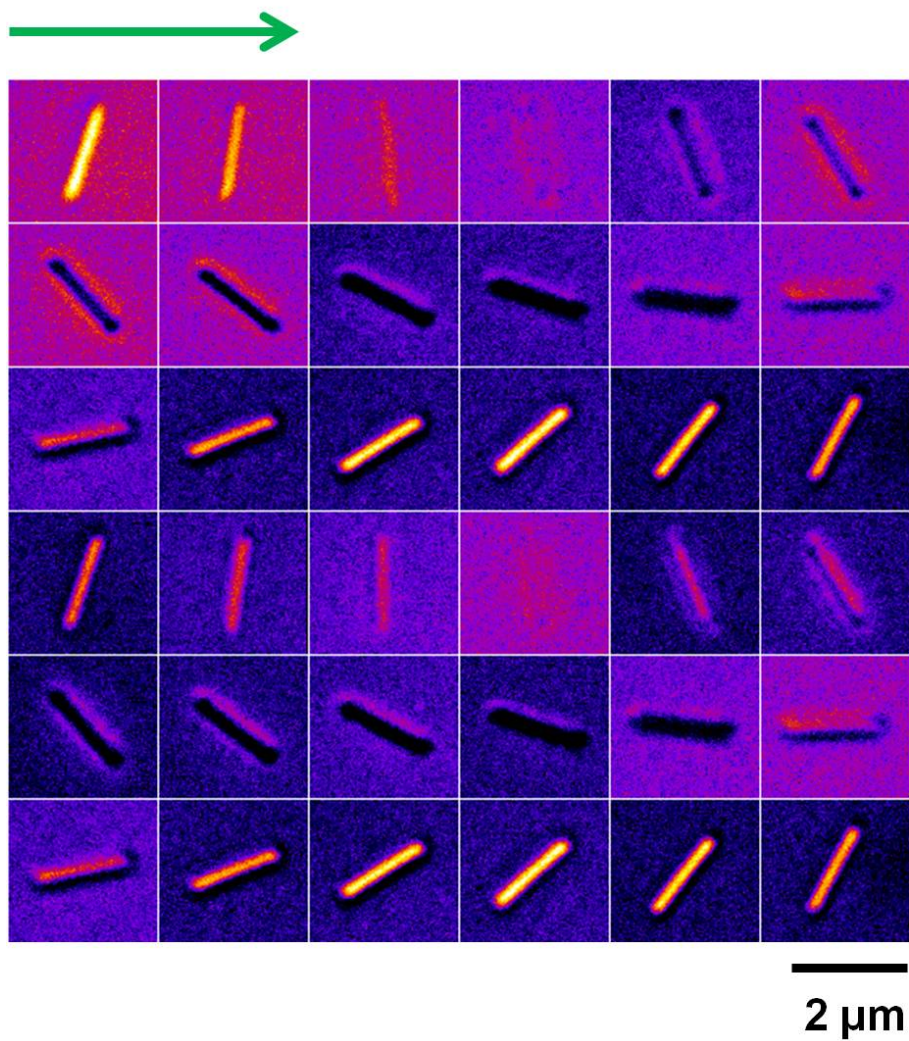


Fig. S7. A complete set of DIC images of the highlighted Au nanowire 2 in Fig. 2 at the excitation wavelength of 640 nm. The image patterns are changed periodically as a function of orientation angle φ from 0° to 360° with an increment of 10° .

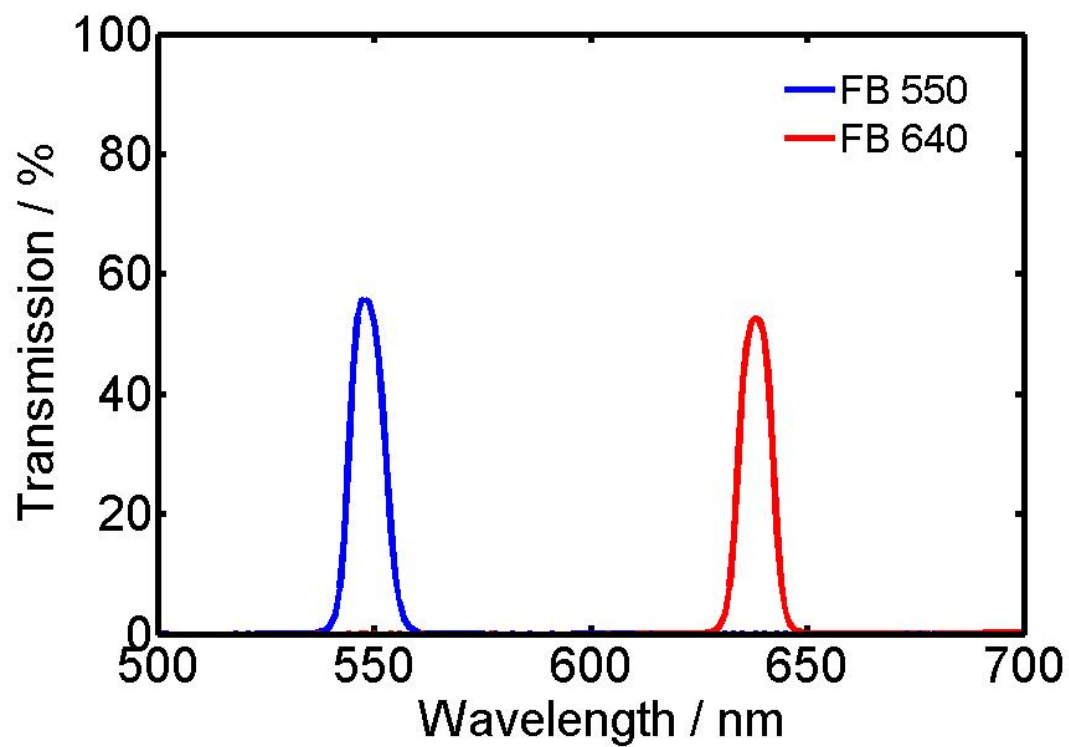


Fig. S8. Transmission of two band-pass filters of 550 nm (blue-curve) and 640 nm (red-curve). The band width (FWHM) is 10 nm for both filters.

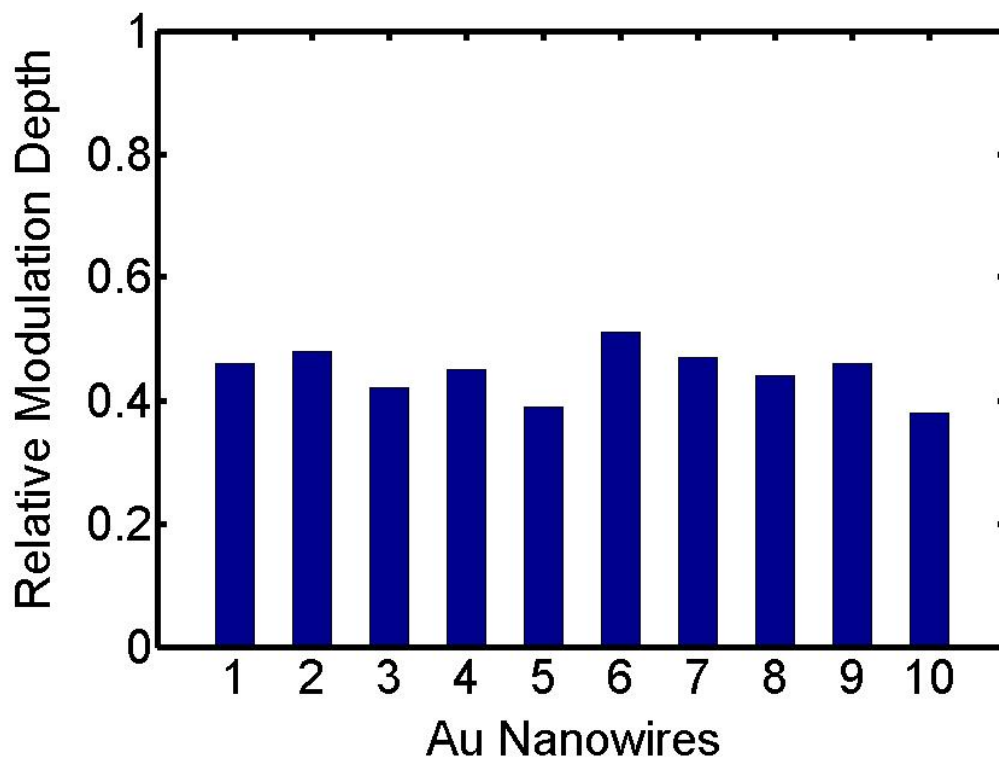


Fig. S9. Relative modulation depth of individual Au nanowires at two SPR wavelengths of 550 nm and 640 nm. When the modulation depth at 550 nm was 1, the relative modulation depth at 640 nm was determined for each nanowire. The average relative modulation depth for 10 nanowires is 0.45.

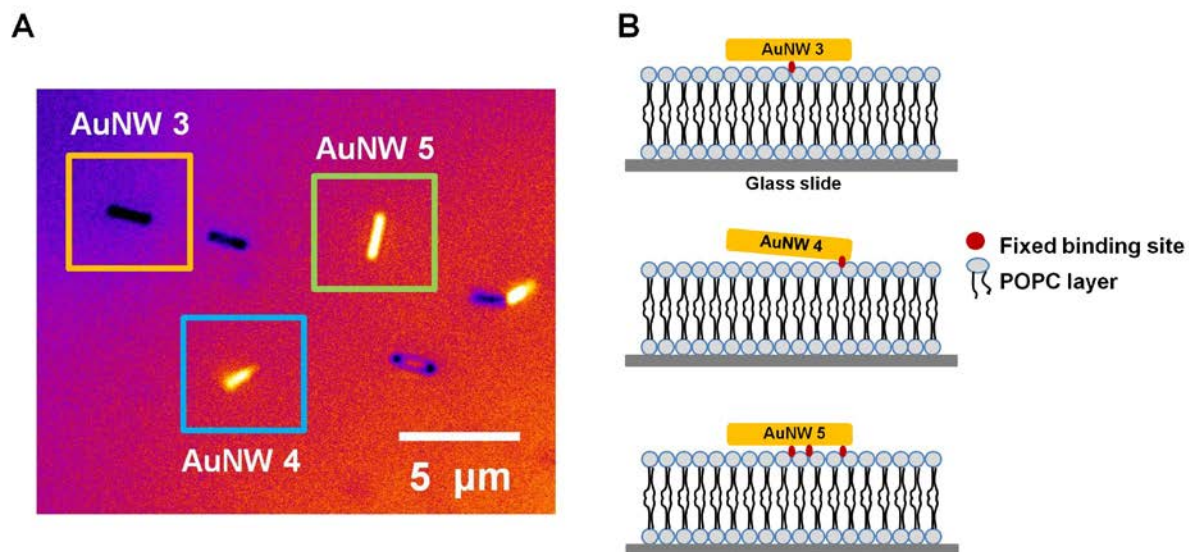


Fig. S10. (A) A DIC image of single Au nanowires bound onto the membrane. (B) Schematics to depict three-distinct conformations of the highlighted Au nanowires on the membrane: One fixed binding site at around its center (Au nanowire 3), one fixed binding site at the end (Au nanowire 4), and multiple fixed binding sites on the membrane (Au nanowire 5).

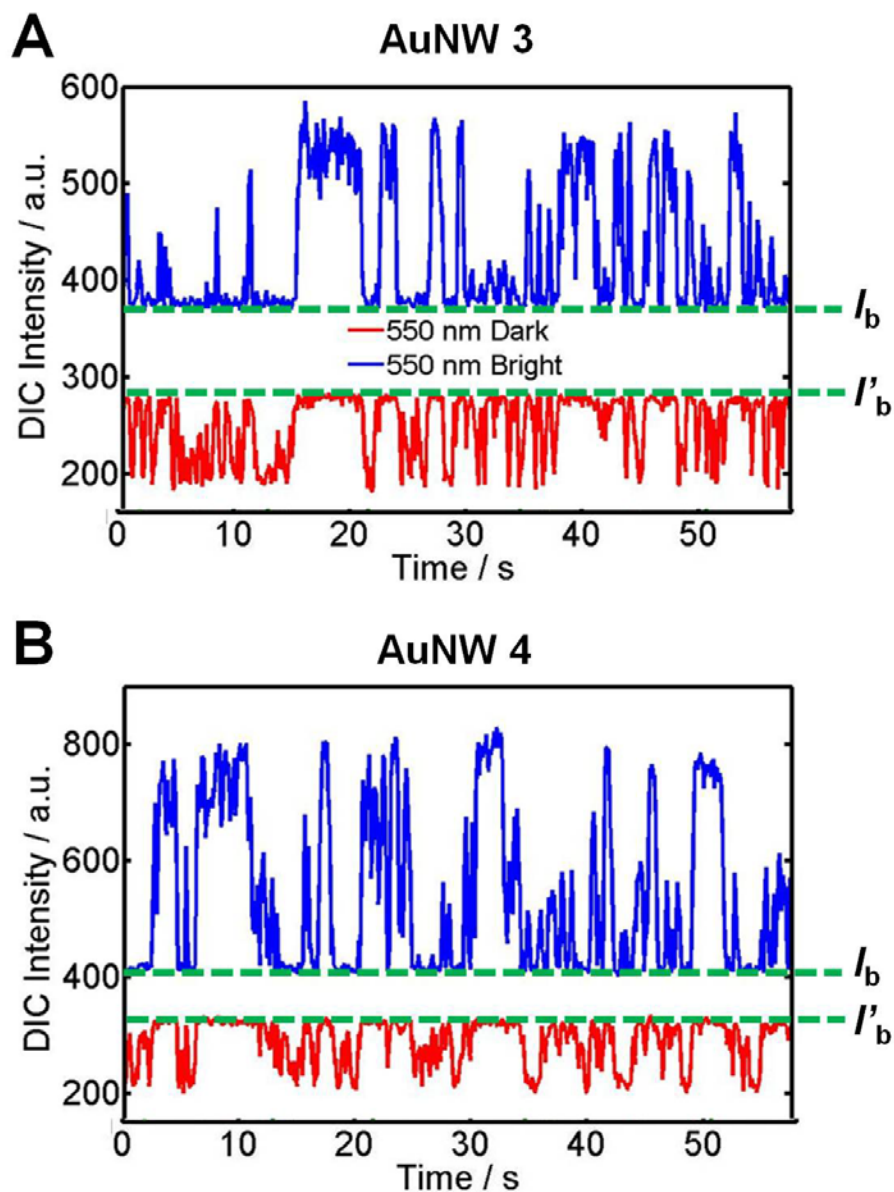


Fig. S11. (A) Change in the bright (blue) and dark (red) intensities of Au nanowire 3 (in Fig. S10A) with one fixed binding site at round its center on the membrane as a function of time. (B) Change in the bright and dark intensities of Au nanowire 4 (in Fig. S10A) with one fixed binding site at the end on the membrane during the rotational dynamics. The green-dotted line indicates the background intensity (I_b).

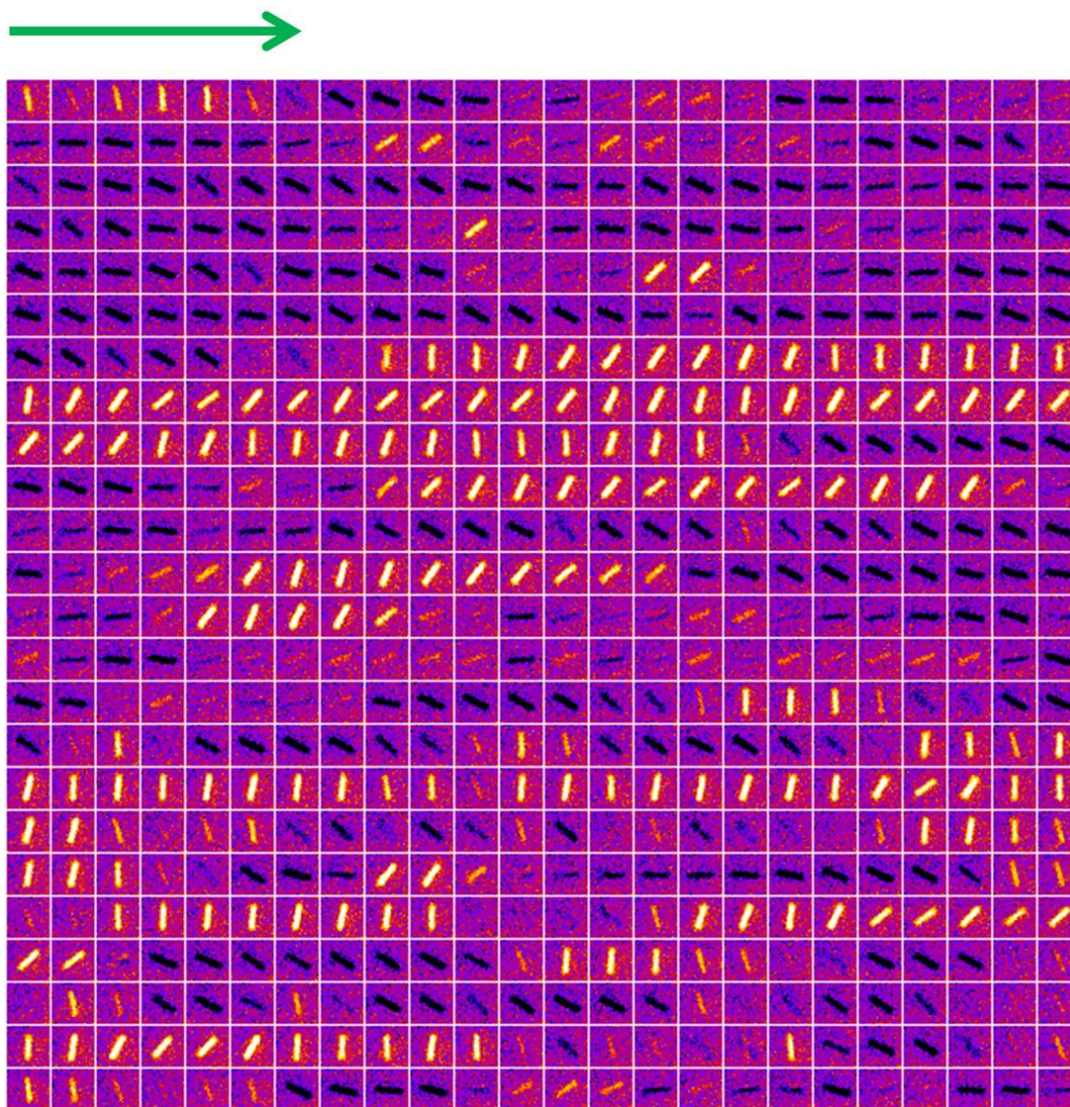


Fig. S12. DIC images of the highlighted Au nanowire 3 in Fig. S10A as a function of time. The successive images are from Movie S1 and are obtained by 550-nm excitation. Temporal resolution is 100 ms.

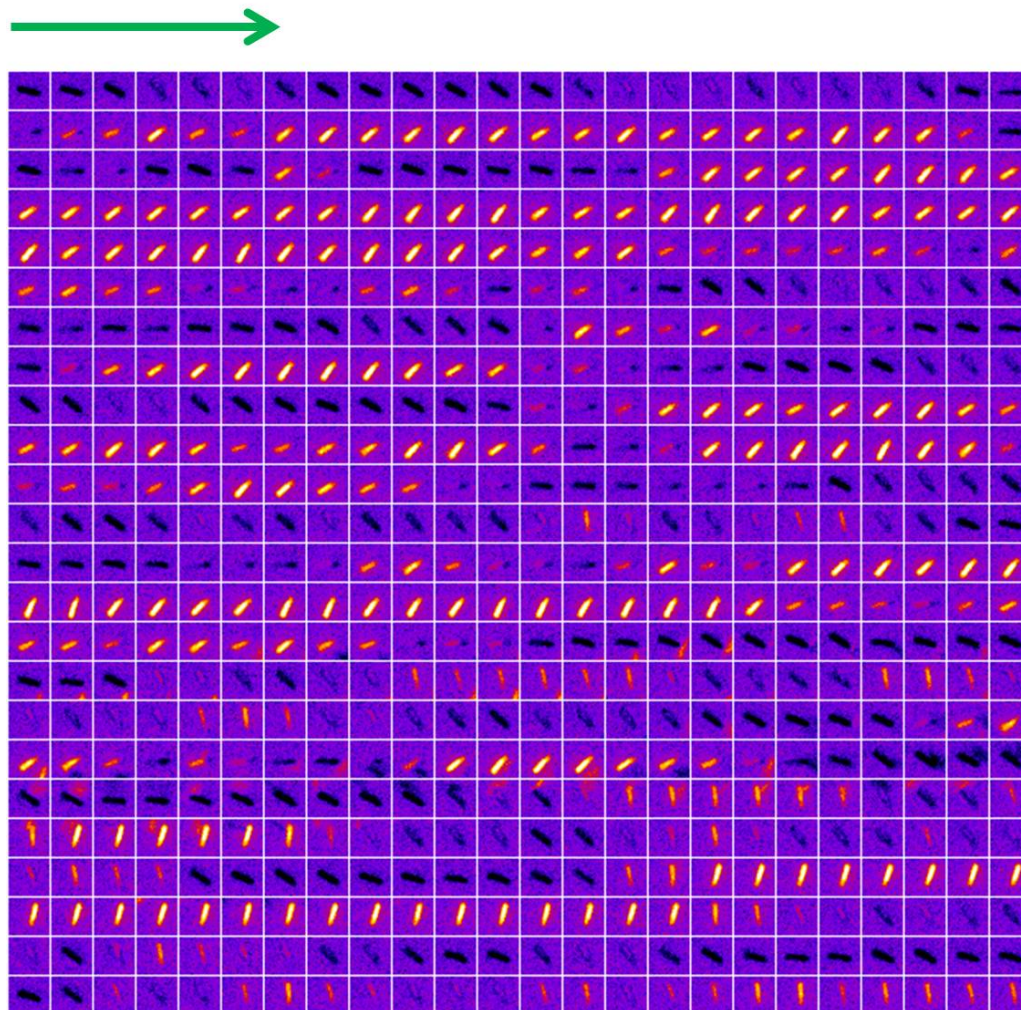


Fig. S13. DIC images of the highlighted Au nanowire 4 in Fig. S10A as a function of time. The successive images are from Movie S2 and are obtained by 550-nm excitation. Temporal resolution is 100 ms.

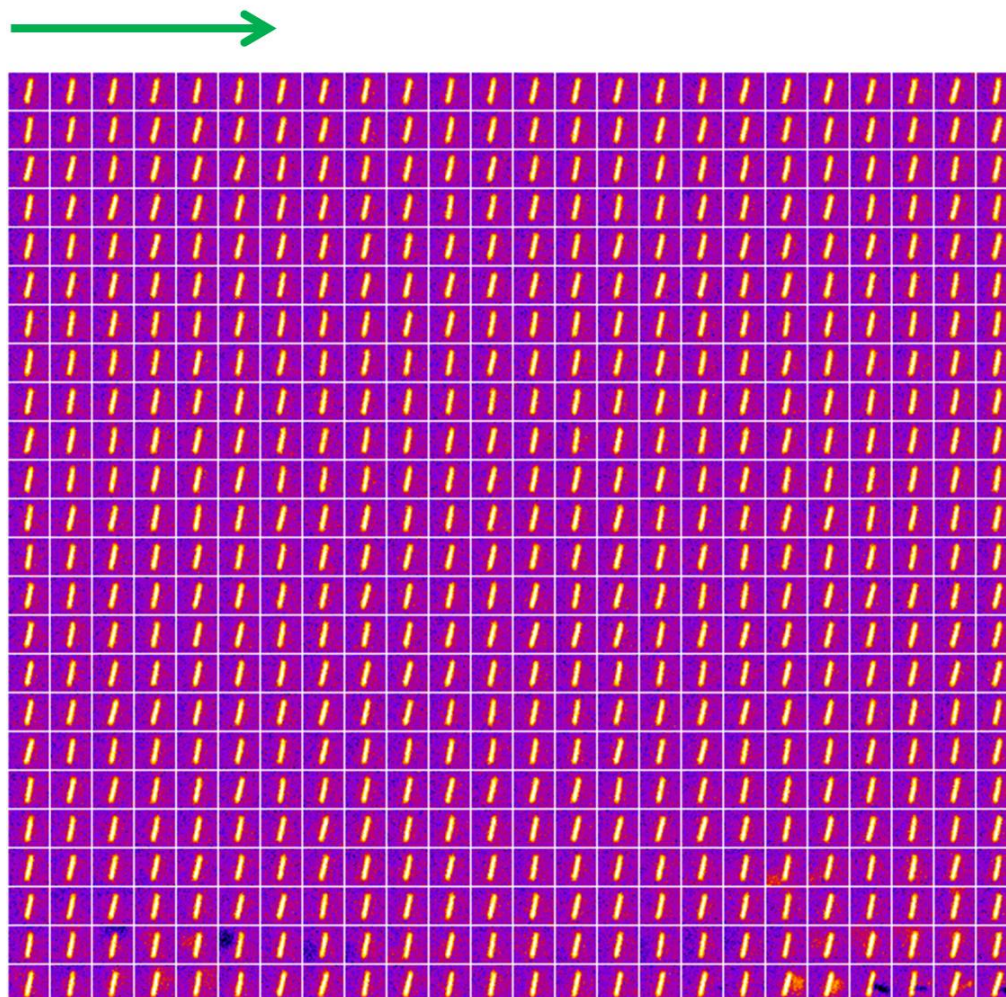


Fig. S14. DIC images of the highlighted Au nanowire 5 in Fig. S10A as a function of time. The successive images are from Movie S3 and are obtained by 550-nm excitation. Temporal resolution is 100 ms.

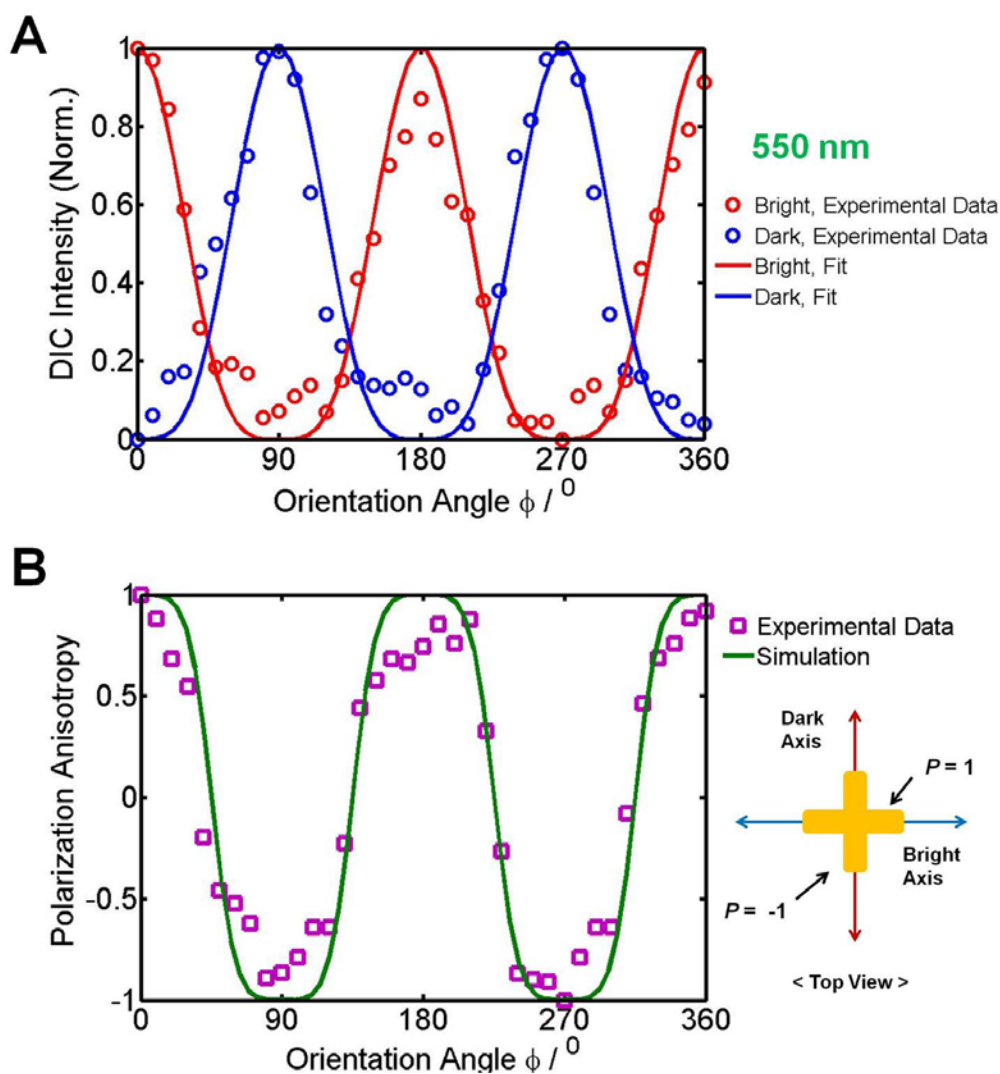


Fig. S15. DIC polarization anisotropy for Au nanowire 2 in Fig. 2 at 550 nm. (A) The normalized bright (red-circle) and dark (blue-circle) intensities for Au nanowire 2 as a function of orientation angle ϕ . The DIC intensities change periodically when the stage rotates by 10° per step. The normalized bright and dark intensities are fitted with $\sin^4(\phi)$ and $\cos^4(\phi)$, respectively. (B) DIC polarization anisotropy P for the nanowire 2. The experimental P values (pink-square) are compared to the calculated P values (green-curve) as a function of orientation angle. Schematic of P values at two special cases ($P=1$ at $\phi=0^\circ$ and $P=-1$ at $\phi=90^\circ$).

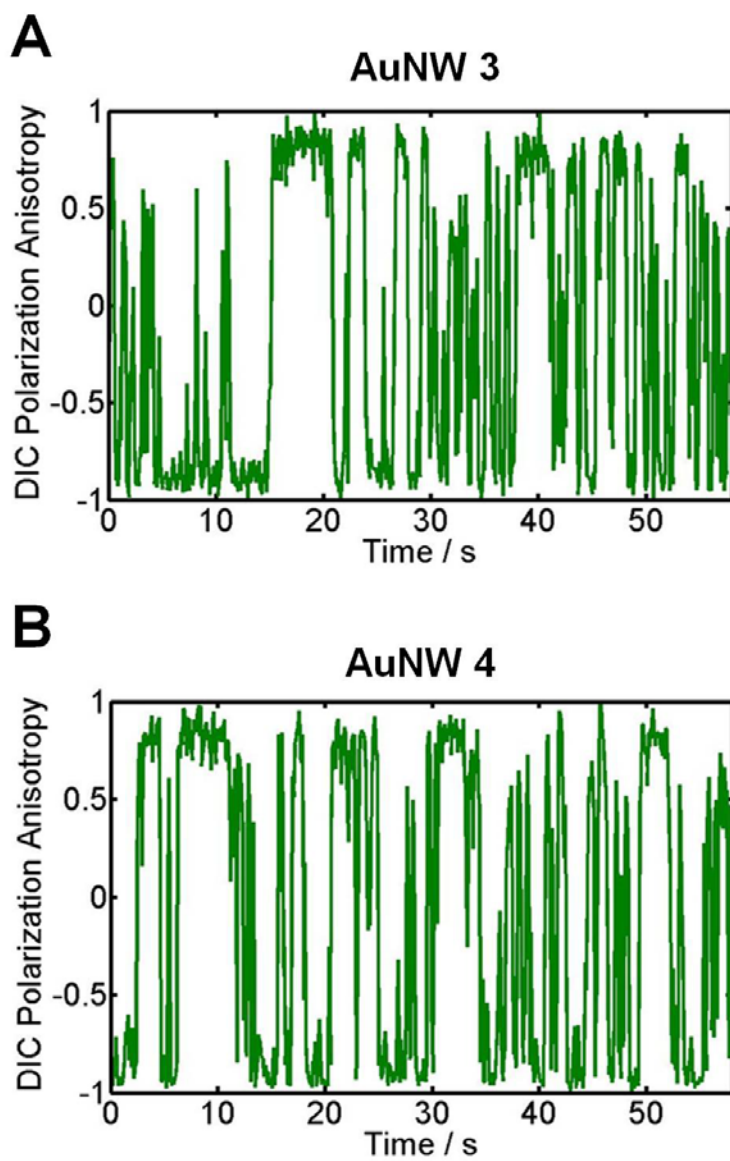


Fig. S16. DIC polarization anisotropy for two Au nanowires 3 and 4 in Fig. S10A as a function of time during the dynamic process.

AuNW 5

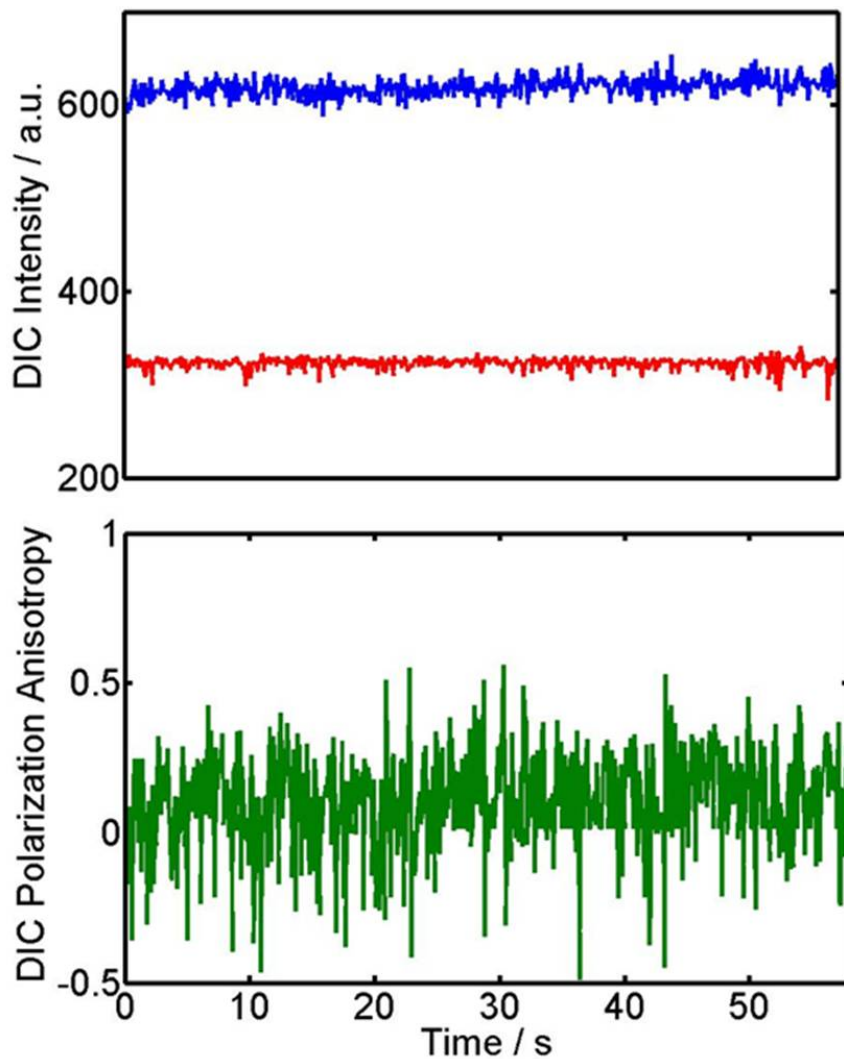


Fig. S17. Change in the bright (blue) and dark (red) intensities of the Au nanowire 5 (in Fig. S10A) with multiple fixed binding sites as a function of time during the dynamic process. The DIC polarization anisotropy for the nanowire 5 is shown below.